Detection of Antipersonnel Landmines Buried in the Clay Soil with UWB Impulse GPR

Gennadiy Pochanin
Dept. of Radiointriscopy
O.Ya.Usikov Institute for Radiophysics and Electronics of the National Academy of Science of Ukraine
Kharkiv, Ukraine
gpp_15@ukr.net

Vadym Ruban
Dept. of Radiointriscopy
O.Ya.Usikov Institute for Radiophysics and Electronics of the National Academy of Science of Ukraine
Kharkiv, Ukraine
ruban@ire.kharkov.ua

Iryna Pochanina
Dept. of Mathematical Physics
O.Ya.Usikov Institute for Radiophysics and Electronics of the National Academy of Science of Ukraine
Kharkiv, Ukraine
irina_pochanina@ukr.net

Tetiana Ogurtsova
Dept. of Radiointriscopy
O.Ya.Usikov Institute for Radiophysics and Electronics of the National Academy of Science of Ukraine
Kharkiv, Ukraine
otn_tati@ukr.net

Vadym Korzh
Dept. of Radiointriscopy
O.Ya.Usikov Institute for Radiophysics and Electronics of the National Academy of Science of Ukraine
Kharkiv, Ukraine
vkrzh@ukr.net

Anatoliy Puzak
Dept. of Radiointriscopy
O.Ya.Usikov Institute for Radiophysics and Electronics of the National Academy of Science of Ukraine
Kharkiv, Ukraine
anatol.puzak@gmail.com

Lorenzo Capineri
dept. of Information Engineering
University of Florence
Florence, Italy
lorenzo.capineri@unifi.it

Timothy Bechtel
dept. of Earth & Environment
Franklin & Marshall College
Lancaster, PA, USA
tbechtel@fandm.edu

Fronefield Crawford
dept. of Physics & Astronomy
Franklin & Marshall College
Lancaster, PA, USA
fcrawfor@fandm.edu

***Abstract*— This paper addresses the challenge of detecting and localizing antipersonnel landmines in clay soil using impulse ultra-wideband (UWB) ground-penetrating radar (GPR). The proposed system employs a 1Tx–4Rx antenna configuration and analyzes the spatial-temporal structure of the received signals. The detection approach is based on contrast filtering and a combined indicator that integrates signal quality (SQ) and correlation coefficient (CC) metrics. Experimental results demonstrate the ability of the system to detect and localize PMN-1 and PMN-2 mines buried in clay soil, highlighting the system's potential for practical applications in humanitarian demining.**

Keywords—landmine, detection, positioning, ground penetrating radar (GPR), ultrawideband (UWB), soil

I. Introduction

Ukraine is considered one of the most heavily contaminated countries worldwide regarding landmines and unexploded ordnance (UXO). According to official estimates, complete clearance of these hazardous remnants may require approximately 700 years. To address this critical issue, the State Emergency Service of Ukraine (SESU) has developed an interactive mapping tool [1] (Fig. 1) that delineates areas potentially affected by explosive objects. This map, regularly updated, includes both confirmed locations of detected ordnance and areas where the presence of explosive items is probable, with risk levels assigned based on SESU data. The map's estimated positional error of up to 30 meters underscores the necessity for the development and deployment of advanced and efficient large-scale mine detection and clearance methods.

The contamination of soil with heavy metals, sulfur, and explosive-derived chemical compounds has rendered large areas of Ukrainian agricultural land unsuitable for cultivation [2], posing an emerging global environmental concern. Consequently, in situ detonation of munitions should be avoided, as it exacerbates soil degradation. Instead, demining efforts should prioritize physical removal of contaminated soil and unexploded ordnance whenever feasible.

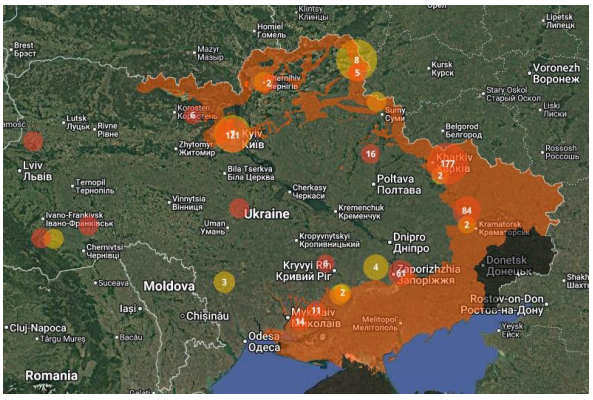

Fig. 1. Interactive map of areas that could potentially be contaminated by explosive objects [1]

A wide range of landmine detection methods has been proposed and experimentally validated. These techniques rely on detecting contrasts in physical properties between buried mines and the surrounding medium [3]. Among these,

The research was carried out with funding from the Ministry of Education and Science within the framework of international scientific and technological cooperation, as outlined in the Protocol of the Fifteenth Meeting of the Joint Ukraine-NATO Working Group on Cooperation in Science and the Environment, dated July 4, 2017, and a letter from O.Ya. Usikov Institute for Radiophysics and Electronics of the National Academy of Sciences of Ukraine dated January 6, 2025_№_65/8/15, regarding the provision of funding for research work under the project of the NATO Program "Science for Peace and Security".

The authors acknowledge the financial support of the NATO/OTAN Science for Peace and Security (SPS) Program for Project G7563-"Innovative Sensor Integration for Remote Landmine Detection" (https://www.natospsdeminingrobots.com/).

ground-penetrating radar (GPR) stands out as a prominent approach, exploiting variations in dielectric permittivity between soil and mine materials to facilitate subsurface detection.

To detect a dielectric object buried beneath the ground, a radar must traverse above it while acquiring GPR data. Processing the recorded profile allows detection and along-track localization, which is standard for all GPR systems. In contrast, GPRs with antenna arrays [4] enable localization in both along-track and cross-track directions.

Recent UAV-based GPR developments enhance buried target detection. Reference [5] presents an autonomous UAV UWB-GPR system with RTK/GPS and SAR processing for high-resolution 3D subsurface imaging. References [6] and [7] combined airborne GPR with magnetometry or GPSAR on micro aerial vehicles, improving cross-range resolution and coherent imaging. Reference [8] demonstrated centimeter-level localization of minimum-metal mines using FMCW radar with circular SAR imaging. A recent patent [9] proposes a compact UAV-suitable multistatic GPR array, enabling efficient multichannel operation with reduced size, weight, and power requirements.

Unlike complex antenna arrays or aperture synthesis, the antenna proposed by us allows real-time determination of a subsurface object's location during GPR movement.

This paper considers and demonstrates the ability to detect and position antipersonnel landmines PMN-1 and PMN-2 using Impulse UWB GPR with a 1Tx–4Rx antenna system.

II. GPR WITH 1TX – 4 RX ANTENNA SYSTEM

A. *Working Principle*

To collect GPR data, we used a 1Tx–4Rx antenna system comprising one transmitting antenna and four receiving antennas, as illustrated in Fig. 2 [10].

The main advantage of the 1Tx–4Rx configuration lies in its ability to determine the 3D coordinates (x,y,z) of a detected object relative to the center of the antenna system [10].

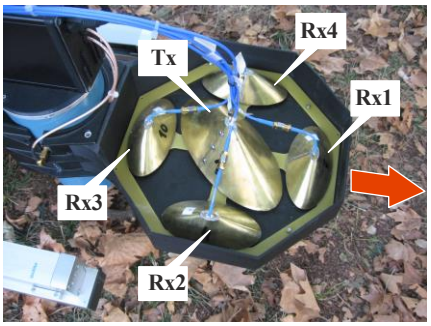

Fig. 2. 1Tx – 4Rx antenna system consisting of one transmitting and four receiving antennas [10]

Under certain conditions, only three or two receivers may receive reflected signals. Papers [11], [12] describe an algorithm that allows finding the coordinates of objects using only three (or even two) Times of Flight (TOFs), measurable with three (or two) receiving channels. Papers [11], [12] demonstrate the possibility of localizing subsurface objects as well.

B. *Results of Experiments. Accuracy of Object Positioning*

To assess the positioning accuracy of the detected to evaluate the positioning accuracy of detected subsurface objects, a series of controlled experiments was conducted (Fig. 3). During these experiments, various test targets—both metallic and plastic—were placed at the nodes of a 10 cm × 10 cm grid on the floor. The antenna system was positioned at a fixed height of 32 cm above the test area to simulate typical survey conditions.

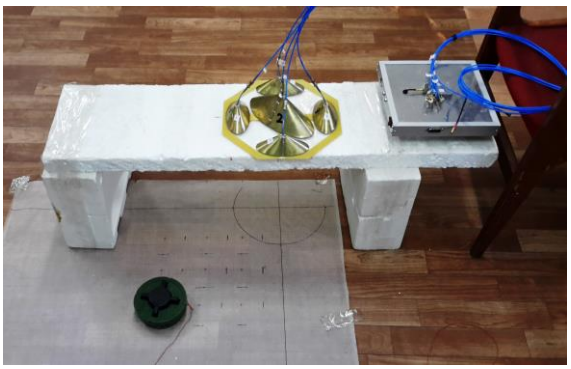

Fig. 3. Experiment on detection and estimation of accuracy of positioning of object on the floor

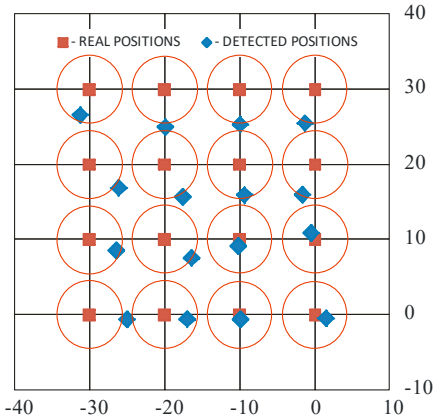

Fig. 4. Actual and detected objects positions. Axes in cm.

The grid of target positions used in the experiments is presented in Fig. 4. The geometric center of the antenna system coinciding with the center of the transmitting antenna was assigned the coordinate origin (X = 0, Y = 0). For the purposes of this study, only the upper-left quadrant of the full observation area was considered. This subsection of the grid had dimensions of 30 cm × 30 cm, corresponding to a 3 × 3 arrangement of grid nodes within the total test field.

The grid of target positions used in the experiments is shown in Fig. 4. The geometric center of the antenna system, which coincides with the center of the transmitting antenna, was defined as the coordinate origin (X = 0, Y = 0). For this study, only the upper-left quadrant of the full observation area was analyzed. This subsection of the grid had dimensions of 30 cm × 30 cm, corresponding to a 4 × 4 arrangement of grid nodes within the total test field.

In Fig. 4, red squares indicate the true positions of the centers of circular objects, while the corresponding red circles represent their actual physical dimensions. Blue squares mark the positions identified through radar signal processing. The results demonstrate successful detection at all 16 grid positions. When the object is located directly beneath the antenna system, the estimated position closely matches the actual center. However, when the object lies outside the central area of the antenna footprint, the detected positions deviate, reflecting signal returns from the lateral surfaces of the object. This effect is attributed to the varying angles of illumination and the relative orientation of the object with respect to the antenna's beam.

It is important to note that all detected positions fall within the circular outlines representing the true dimensions of the objects. This indicates that the positional accuracy of the impulse GPR is sufficient for practical applications. From the perspective of subsequent high-resolution imaging, such as holographic radar scanning, the initial localization provided by the impulse GPR serves as an adequate starting point for detailed shape reconstruction and target characterization.

III. Algorithms of Radar Data Processing

Data processing consists of three steps: background removal (which is usual for GPR), correlation algorithm (which allows determining TOFs for signals reflected by subsurface objects), and spatial filtering (which additionally filters subsurface objects based on information about the trajectory of GPR movement).

A. Background Removal

In conventional GPR data processing, background removal is often performed by averaging the signal across the entire radar profile and subtracting this averaged trace from each individual trace, a technique commonly referred to as average trace subtraction (ATS) or mean subtraction (MS) [3], [13], [14]. Beyond ATS, several studies have critically reviewed this and related approaches including median filtering, singular value decomposition (SVD), principal component analysis (PCA), and independent component analysis (ICA) for their effectiveness in enhancing the signal-to-clutter ratio under varying soil moisture conditions [15]. Additionally, in GPR processing software such as REFLEXW, simple background removal via average trace subtraction is typically the first step in clutter mitigation, especially against horizontal, coherent noise like ringing [16].

The paper [17] presents an advanced approach to mitigate the influence of background on the detection of subsurface objects.

A central objective of this study is the identification and elimination of interference sources that degrade the reliability of subsurface object detection. The primary sources of interference considered include: (i) direct electromagnetic coupling between transmitting and receiving radar antennas; (ii) reflections from structural elements of the robotic platform; (iii) surface reflections from the ground; and (iv) instability of the GPR signal, particularly due to temperature-induced drift occurring during extended scanning sessions. Addressing these factors is essential for enhancing the accuracy and robustness of the detection algorithm.

To mitigate the aforementioned sources of interference, a series of measurements were conducted with the robotic platform suspended in air, at a sufficient height above the ground. This configuration ensured that any signals resulting from subsurface reflections would arrive significantly later than those originating from the platform structure, enabling clear identification and subtraction of structural reflections. The recorded signals were also utilized to compensate for temperature-induced drift in the radar response, as well as to suppress direct coupling effects between the transmitting and receiving antennas.

A distinctive feature of the advanced algorithm [18] is the following. The background removal procedure consists of the following steps: selection of a time window preceding the surface reflection; application of an optimization procedure to determine time drift caused by temperature variations; alignment of the two signals; and subtraction of the background signal from the received one. This process is called “adjusted subtraction” and is performed independently for all four receiving channels.

The need to remove reflections from the soil surface arises from the fact that these signals arrive at the receiver almost simultaneously with reflections from shallowly buried objects, making it difficult to determine the actual arrival time of the target response. Reflections from the surface can also be eliminated using a similar approach as described above. However, instead of using pre-recorded background signals, we utilized signals collected a few centimeters ahead of a known target. The algorithm was tested on real data and demonstrated its effectiveness.

As a result of the refined subtraction procedures applied to both the background signal and the reflection from the soil surface, two key improvements were achieved. First, the dominant background signal, which can obscure weaker reflections from subsurface targets, was successfully removed. Second, the waveform of the surface reflection was significantly improved, resulting in clearer separation between surface and near-surface responses. These enhancements contributed to more robust and consistent Pearson correlation values, facilitating a more reliable determination of the TOF of the reflected signals.

B. Correlation Algorithm. Selecting Object Coordinates

Experimental investigations revealed that multiple signal reflections and the corresponding TOF measurements are registered at each receiver, even in scenarios involving a single subsurface object. This phenomenon arises due to several factors, including artifacts introduced by the correlation-based TOF estimation algorithm, variations in the UWB signal waveform depending on the object's position and orientation relative to the antenna system, as well as potential signal interference and environmental or system noise. The presence of these multiple TOFs introduces ambiguity in object localization and can lead to erroneous coordinate determination.

Addressing this challenge, an approach is presented in the paper [18]. It proposes a set of criteria for identifying and

eliminating spurious TOF detections and the associated phantom object coordinates.

The coordinate determination algorithm was enhanced with a set of formalized criteria designed to distinguish true object positions from false detections (phantoms). Experimental validation demonstrated that applying five such criteria enable reliable detection of the PMN-4 simulant in a sand test bed. Moreover, the estimated coordinates achieved spatial accuracy exceeding the target's physical dimensions—that is, the localization error was smaller than the diameter of the object.

C. Spatial Filtering. Automatic Detection.

The automatic detection algorithm was evaluated using both previously collected datasets and real-time data acquired during active sounding. This dual approach allowed for assessing the algorithm's robustness under controlled as well as dynamic conditions

Fig. 5. PMN4 (on the left) is burried (on the right)

For the experimental validation of the detection algorithm, three types of buried objects were employed: a metal tin, a surrogate representing the PMN-4 mine type, and a simulant mimicking the physical characteristics of the PMN-1 mine. These objects were selected to represent a range of material compositions and geometries relevant to real-world demining scenarios

Figures 6–8 present the results of spatial filtering performed using the detection algorithm described in [19]. In the case of the metal tin, multiple candidate positions were identified, providing several approach options for a mobile robotic platform. Notably, the detection and corresponding generation of the "ALARM" signal occurred when the object was located approximately 10 cm ahead of the center of the antenna system along the OX axis, which intersected the object's position. This behavior reflects the algorithm's responsiveness prior to direct antenna alignment with the target.

As observed in the experiment, the PMN-4 surrogate was positioned approximately 10 cm to the right of the antenna system's central axis (Fig. 7). As a result, the number of detected positions was reduced compared to the case with the metal tin (fewer markers are visible in Fig. 7 than in Fig. 6). Nevertheless, the PMN-4 was successfully detected and localized. The "ALARM" signal was generated when the OX axis of the antenna system intersected the position of the mine simulant, while the robotic platform remained at a safe distance.

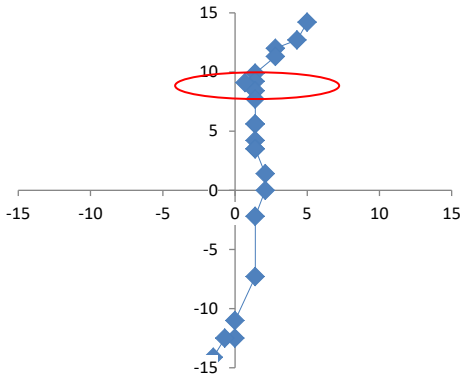

Fig. 6. Track of PMN4 simulant after object selection procedure. Red circle means position of detection and sending "ALARM" message to ROS..

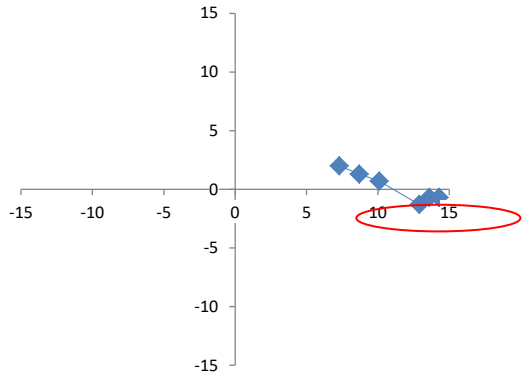

Fig. 7. Track of PMN4 simulant after object selection procedure. Red circle means position of detection and sending "ALARM" message to ROS..

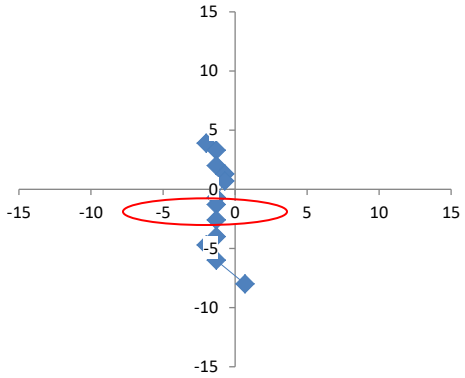

Fig. 8. Track of PMN-4 simulant after object selection procedure. Red circle means position of detection and sending "ALARM" message to ROS.

The detection of the PMN-1 simulant also demonstrated a sufficient level of reliability (Fig. 8). A considerable number of candidate positions were identified, indicating stable performance of the detection algorithm. In this case, the "ALARM" signal was triggered at an appropriate moment, when the center of the impulse GPR antenna system directly aligned with the object. This response ensures effective and safe localization suitable for robotic navigation and further investigation.

IV. Results of Experiments

Before starting the experiments, we prepared the test field by removing all metal objects and pebbles.

A. *Measurements on an Empty Training Site*

Three scans were performed with an offset of 30 cm.

During the first scan, the robot moved near the left edge of the test site; during the second — in the center; during the third — near the right edge of the test site (Fig. 9a).

The collected data were processed using a correlation procedure. The results of the processing, using a reflection from a metal sheet as the reference signal, are illustrated in Fig. 9b. The coordinates of all "detected targets" from three scans are marked as small spots. It is important to note that there are no actual targets in the test field; instead, what has been detected are artifacts that occurred during the data processing.

In the implemented detection algorithm [18], two principal indicators are employed: the normalized signal energy (SQ) and the correlation coefficient (CC). The SQ metric quantifies the total signal energy within a predefined time window by summing squared amplitudes, serving as an indicator of potential target presence. The CC metric assesses the similarity between the received waveform and a calibrated reference response from a metal plate, thereby enabling accurate determination of the TOF. These two complementary metrics collectively inform the assessment of detection probability (PD), balancing energy-based detection with waveform consistency.

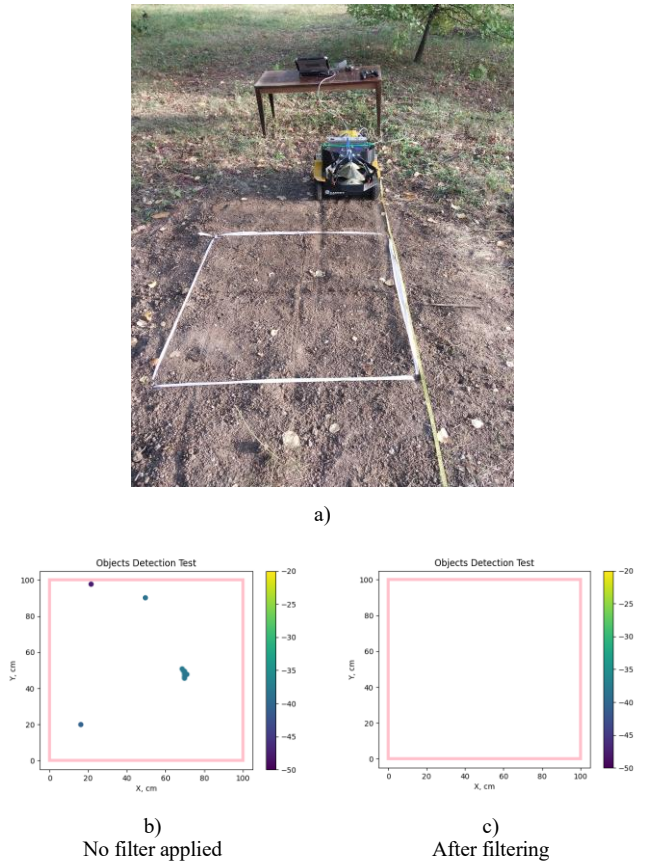

a)

b) No filter applied

c) After filtering

Fig. 9. Empty test site (a); result of GPR scanning (b); result of filtering (c)

To evaluate detection performance, we selected nine threshold levels for the normalized energy coefficient (SQ), ranging from 0 to 0.08, and five threshold levels for the correlation coefficient (CC), ranging from 0 to 0.5. For each combination of these thresholds, we assessed whether object detection occurred and recorded the corresponding counts of true and false detections within a predefined area of interest.

After spatial filtering and selecting the necessary thresholds, all artifacts were removed from the test field image (Fig. 9c).

B. *Measurements at the test site with PMN-1 and PMN-4*

At the next step, two simulants of landmines, PMN-4 and PMN-1, were buried in the soil. Their coordinates in cm were (25, 75, -5) for PMN-4 and (75, 75, -10) for PMN-1.

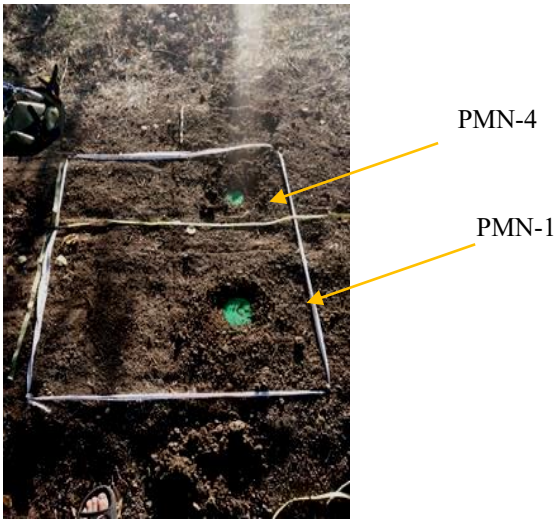

Fig. 10. Simulants of the PMN-1 and PMN-4 landmines on the test field before being buried

During the landmine installation and recent scanning with the robotic platform, soil was compacted in certain areas. The following scan produced the image of the test field shown in Fig. 11a.

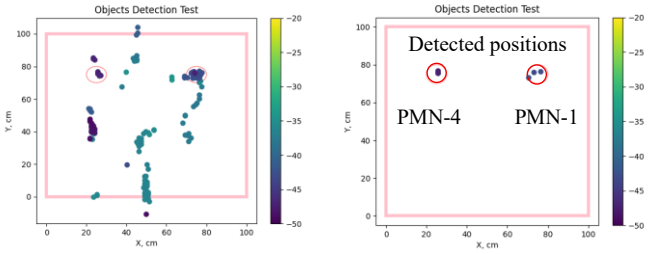

a) b)

Fig. 11. Results of investigation of the test area with buried simulants of the PMN-1 and PMN-4 landmines

After data processing, all false detections were removed, and the correct detections were located within the circles representing the objects' diameters. The resulting image (Fig. 11b) shows small blue spots corresponding to positions detected during GPR scanning (two for the PMN-4 and three for the PMN-1). Red circles mark the burial locations of the landmine simulants.

Data collected without analog accumulation were used for processing.

Target selection thresholds:

- According to the correlation coefficient – 0.25.
- According to the energy coefficient - 0.05.

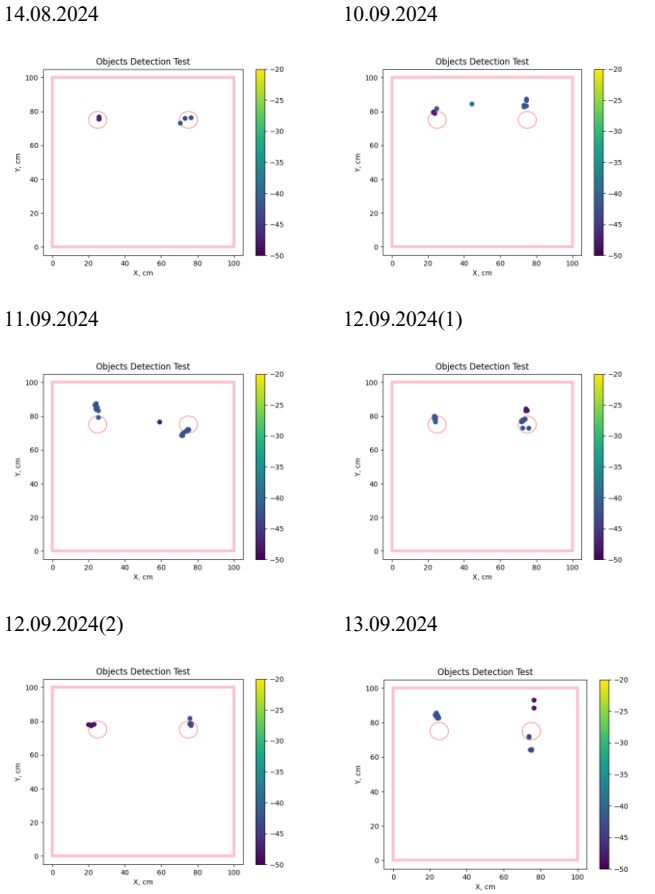

Fig. 12. Results of GPR sounding data processing on a 100x100 cm field with PMN-1 (on the right) and PMN-4 (on the left)

CONCLUSIONS

This study has demonstrated the feasibility of using impulse ultra-wideband ground-penetrating radar (GPR) with a 1Tx–4Rx antenna system for detecting and positioning antipersonnel landmines buried in clay soil. The system reliably located simulants of PMN-1 and PMN-4 mines with spatial accuracy better than the physical dimensions of the targets.

Recent advancements in data processing have led to significant improvements. The introduction of advanced background removal techniques reduces the impact of interference and surface reflections. Additionally, a strong correlation-based time-of-flight detection algorithm, combined with spatial filtering, has greatly reduced false alarms and enhanced the reliability of localization.

The ability to provide accurate initial localization supports further high-resolution imaging techniques, such as holographic radar scanning, facilitating detailed target identification and characterization. The proposed system and algorithms thus represent a promising tool for humanitarian demining applications, potentially accelerating the safe clearance of contaminated land areas.

REFERENCES

[1] Demining Ukraine," *Dsns.gov.ua*, 2025. https://mine.dsns.gov.ua

[2] Maia Orel, "Ammunition against fertile soils: why Ukraine can lose the status of the breadwinner of the world," hromadske, Aug. 04, 2023. https://hromadske.ua/ru/posts/boepripasy-protiv-plodorodnyh-pochv-pochemu-ukraina-mozhet-poteryat-status-kormilicy-mira

[3] David John Daniels, D. J. Daniels, and Institution Of Electrical Engineers, *Ground penetrating radar*. London: The Institution Of Electrical Engineers, 2004.

[4] M. Sato, Y. Hamada, X. Feng, F.-N. Kong, Z. Zeng, and G. Fang, "GPR using an array antenna for landmine detection," *Near Surface Geophysics*, vol. 2, no. 1, pp. 7–13, Dec. 2003, doi: https://doi.org/10.3997/1873-0604.2003011.

[5] M. Garcia-Fernandez, Y. Alvarez-Lopez, and F. Las Heras, "Autonomous Airborne 3D SAR Imaging System for Subsurface Sensing: UWB-GPR on Board a UAV for Landmine and IED Detection," *Remote Sensing*, vol. 11, no. 20, p. 2357, Oct. 2019, doi: https://doi.org/10.3390/rs11202357

[6] Pérez Cerquera, Manuel & Colorado, Julian & Mondragón, Iván. (2017). UAV for Landmine Detection Using SDR-Based GPR Technology. 10.5772/intechopen.69738.

[7] R. Bähnemann *et al.*, "Under the Sand: Navigation and Localization of a Micro Aerial Vehicle for Landmine Detection with Ground-Penetrating Synthetic Aperture Radar," *Field Robotics*, vol. 2, no. 1, pp. 1028–1067, Mar. 2022, doi: https://doi.org/10.55417/fr.2022034.

[8] M. Schartel, R. Burr, Rik Bähnemann, W. Mayer, and C. Waldschmidt, "An Experimental Study on Airborne Landmine Detection Using a Circular Synthetic Aperture Radar," *arXiv (Cornell University)*, Jan. 2020, doi: https://doi.org/10.48550/arxiv.2005.02600.

[9] N. Reginald BeerSteven BondPeter C. HaugenJacob TruebloodBrian Matthew Wihl "UAV ground penetrating radar array" Patent (WO2021155343A2) published by 2021-08-05.

[10] V. Ruban *et al.*, "Object coordinate determination by the impulse GPR with a Tx + 4Rx antenna system," Oct. 2022, doi: https://doi.org/10.1190/gpr2022-120.1.

[11] G. P. Pochanin *et al.*, "Measurement of Coordinates for a Cylindrical Target Using Times of Flight from a 1-Transmitter and 4-Receiver UWB Antenna System," *IEEE Transactions on Geoscience and Remote Sensing*, vol. 58, no. 2, pp. 1363–1372, Oct. 2019, doi: https://doi.org/10.1109/tgrs.2019.2946064

[12] V. Ruban *et al.*, "Determining of the Subsurface Object Coordinates Using 1Tx + 4Rx Antenna System at Incomplete Set of Reflections," pp. 1–4, Jul. 2023, doi: https://doi.org/10.1109/iwagpr57138.2023.10329138.

[13] E. A. Rashed, "GPR background removal using a directional total variation minimisation approach," *Journal of Geophysics and Engineering*, vol. 12, no. 6, pp. 897–908, Oct. 2015, doi: https://doi.org/10.1088/1742-2132/12/6/897.

[14] L. Liu et al., "GPR Clutter Removal Based on Weighted Nuclear Norm Minimization for Nonparallel Cases," Sensors, vol. 23, no. 11, pp. 5078–5078, May 2023, doi: https://doi.org/10.3390/s23115078.

[15] P. Sharma, B. Kumar, D. Singh, and S. P. Gaba, "Critical Analysis of Background Subtraction Techniques on Real GPR Data," *Defence Science Journal*, vol. 67, no. 5, p. 559, Sep. 2017, doi: https://doi.org/10.14429/dsj.67.10048.

[16] https://www.sandmeier-geo.de/Download/gpr_2d_import_processing.pdf?utm_source=chatgpt.com

[17] L. Capineri *et al.*, "Background Removal for the Processing of Scans Acquired with the, 'UGO-1st', Landmine Detection Platform," *2019 PhotonIcs & Electromagnetics Research Symposium - Spring (PIERS-Spring)*, Jun. 2019, doi: https://doi.org/10.1109/piers-spring46901.2019.9017781

[18] V. Ruban et al., "Automatic Detection of Subsurface Objects with the Impulse GPR of the UGO-1st Robotic Platform," 2020 IEEE Ukrainian Microwave Week (UkrMW), Sep. 2020, doi: https://doi.org/10.1109/ukrmw49653.2020.9252816

[19] Tetiana Ogurtsova *et al.*, "Criteria for Selecting Object Coordinates at Probing by the Impulse UWB GPR with the '1Tx + 4Rx' Antenna System," pp. 161–164, Sep. 2018, doi: https://doi.org/10.1109/uwbusis.2018.8520088.